PRIFYSGOL ABERYSTWYTH UNIVERSITY

Aberystwyth University

Assessing the impact of pulsed-irradiation procedures on the thermally transferred OSL signal in quartz

Chapot, Melissa; Duller, G. A. T.; Roberts, H. M.

Published in:
Radiation Measurements

DOI:
10.1016/j.radmeas.2014.04.003

Publication date:
2014

Citation for published version (APA):
Chapot, M., Duller, G. A. T., & Roberts, H. M. (2014). Assessing the impact of pulsed-irradiation procedures on the thermally transferred OSL signal in quartz. *Radiation Measurements*, *65*, 1-7. https://doi.org/10.1016/j.radmeas.2014.04.003

General rights
Copyright and moral rights for the publications made accessible in the Aberystwyth Research Portal (the Institutional Repository) are retained by the authors and/or other copyright owners and it is a condition of accessing publications that users recognise and abide by the legal requirements associated with these rights.

• Users may download and print one copy of any publication from the Aberystwyth Research Portal for the purpose of private study or research.
• You may not further distribute the material or use it for any profit-making activity or commercial gain
• You may freely distribute the URL identifying the publication in the Aberystwyth Research Portal

Take down policy
If you believe that this document breaches copyright please contact us providing details, and we will remove access to the work immediately and investigate your claim.

tel: +44 1970 62 2400
email: is@aber.ac.uk

Download date: 08. May. 2023

Postprint of paper published in Radiation Measurements:
Chapot, M. S., Duller, G. A. T. and Roberts, H. M. (2014). Assessing the impact of pulsed-irradiation procedures on the thermally transferred OSL signal in quartz. Radiation Measurements 65, 1-7. (doi:10.1016/j.radmeas.2014.04.003)

Assessing the impact of pulsed-irradiation procedures on the thermally transferred OSL signal in quartz

M.S. Chapot,* G.A.T. Duller, and H.M. Roberts

Department of Geography and Earth Sciences, Aberystwyth University, Aberystwyth, SY23 3DB, U.K.
**corresponding author (msj1@aber.ac.uk)*
Tel: 44 (0) 1970 622606

Abstract

Thermally transferred optically stimulated luminescence (TT-OSL) dating protocols have been suggested as a means of extending the age range of luminescence dating. Several studies demonstrate that TT-OSL signals increase with large radiation doses (>2000 Gy) and yet, few studies report older TT-OSL ages (>400 Gy) in agreement with independent absolute age control. In one such study, agreement with independent chronology was only achieved for the old samples by implementing a pulsed-irradiation procedure. Pulsed-irradiation is suggested to compensate for dose rate dependent competition effects by dividing the laboratory irradiation into discrete irradiation steps interspersed with heat treatments. However, every inter-step heat treatment has the potential to anneal part of the TT-OSL dating signal. This study compares constant- and pulsed-irradiation TT-OSL protocols and investigates the degree of partial thermal annealing. The results suggest that almost all of the difference in outcome between constant- and pulsed-irradiation protocols can be explained by partial annealing of the TT-OSL signal rather than by competition effects. Partial annealing distorts the laboratory dose response curve but has no impact on the natural signal, resulting in unreliable equivalent dose estimates. This means that pulsed-irradiation procedures may not be viable for TT-OSL dating measurements. Future studies implementing pulsed-irradiation procedures should carefully consider the extent to which inter-step thermal treatments partially anneal the signal.

Keywords

TT-OSL, pulsed-irradiation, partial annealing, Chinese Loess Plateau, maximum age, fine-grain quartz

1. Introduction

The thermally transferred optically stimulated luminescence signal (TT-OSL) from quartz has been observed to grow to larger laboratory radiation doses than the more commonly used optically stimulated luminescence (OSL) signal (Wang et al., 2006b), thus giving the TT-OSL signal the potential to extend the age range of luminescence dating. The first study to use the TT-OSL signal for dating (Wang et al., 2006a) demonstrated agreement between TT-OSL and OSL equivalent doses (D_e) up to ~400 Gy. However, sample IEE424 from near the Brunhes-Matuyama (B/M) palaeomagnetic reversal obtained a D_e value of 1460 ± 62 Gy resulting in an age estimate of only 474 ± 27 ka (Wang et al., 2006a), far from the age obtained using Ar-Ar dating (775.6 ± 1.9 ka; Coe et al., 2004).

The severe age underestimation of this sample led Wang et al. (2006a) to investigate pulsed-irradiation protocols. Using a protocol that divides laboratory irradiation into ~150 Gy irradiation steps separated by a 240 °C cut heat, Wang et al. (2006a) were able to obtain equivalent doses that resulted in ages agreeing with the B/M age for sample IEE424 and for three other samples taken from near the B/M boundary. Although this suggested that a pulsed-irradiation protocol was necessary for the older samples in that study, subsequent investigations and applications of the TT-OSL signal have used only constant-irradiation protocols. In agreement with Wang et al. (2006a), most of these subsequent investigations have been unable to successfully date an older sample (>400 Gy) with independent age control (Duller and Wintle, 2012; Thiel et al., 2012). However, one recent investigation using constant irradiation has reported two older ages (~700 and ~1000 ka) in agreement with independent U-Pb ages and palaeomagnetic reversals (Pickering et al., 2013).

Pulsed-irradiation was initially proposed by Bailey (2004) as a means of compensating for differences between dose rates in nature and in the laboratory. This work was on simulations of modelled OSL data, but there has been limited application to real samples. The assumption that natural and laboratory radiation result in the same trapped charge distribution is fundamental to luminescence dating, but the two radiation sources have known differences. Natural dose rates are typically 1-4 Gy/ka and are comprised of a mixed radiation field including alpha, beta, and gamma radiation, whereas laboratory dose rates are typically of the order of 10^9 Gy/ka and are comprised of a single radiation type (most commonly beta radiation).

Due to the complexity of the charge distribution in quartz grains, the difference in magnitude between natural and laboratory dose rates could result in either age underestimation or overestimation (Qin and Zhou, 2009). For example, if the quartz grain has an abundance of temporally unstable electron traps (such as those associated with the 110 °C thermoluminescence peak), constant-laboratory irradiation could potentially underestimate the natural signal. In nature, these shallow traps capture electrons slowly due to the low dose rates and these electrons are then released due to the long duration of the irradiation and the short lifetime of charge in this trap at room temperature. The result is that these traps are effectively empty such that they can compete for each free electron in the conduction band. During the short, high dose rate laboratory irradiations these shallow traps collect electrons more rapidly than they escape, resulting in a higher equilibrium concentration than in nature and therefore reducing the competition for electrons with the deeper traps used for dating. This results in signals from laboratory doses that are brighter than signals from equivalent natural doses, and therefore results in age underestimation.

The opposite effect can occur if the quartz grain has an abundance of temporally unstable electronic hole traps. In this instance, competition for electrons during recombination would be greater for laboratory irradiation due to a higher concentration of electronic holes in alternative recombination centres, resulting in the natural signal being brighter than an equivalent laboratory signal and therefore leading to age overestimation (Bailey, 2004). Pulsed-irradiation divides the laboratory irradiation dose into smaller irradiation steps and heats the sample between steps. The thermal treatments between steps are designed to deplete the temporally unstable traps and thus make laboratory competition effects in the quartz crystal similar to those which occur due to the low radiation dose rates received in nature.

Although pulsed-irradiation has the potential to address charge competition, an additional, unwanted effect of the protocol may be to partially anneal the target signal, if the thermal treatments are carried out at temperatures which are too high. Every inter-step thermal treatment during the protocol has the potential to remove a certain percentage of the signal used for dating. This additional effect could result in undesirable changes to the age estimate, unless the partial annealing is negligibly small.

This study explores the use of pulsed-irradiation for TT-OSL protocols by observing the difference in outcome between constant- and pulsed-irradiation protocols, and then investigates the relative influence of any partial annealing caused by the heat treatments between irradiation steps.

2. Sample description and instrumentation

Sample PT2, collected from the top of L3 at the Luochuan section of the Chinese Loess Plateau, was used for all of the measurements reported in this paper. This section is the same as that analysed by Wang et al. (2006a). The sample was collected as a small block wrapped in black plastic. Once in the darkroom conditions of the laboratory, the exterior of the block was removed and the remaining material was treated with 10% dilution by volume of concentrated HCl and 20 vols H_2O_2 until no continued reaction could be identified. The material was then settled in sodium oxalate using Stokes Law to obtain the 4-11 μm fraction, treated with H_2SiF_6 for 14 days to remove feldspar (Roberts, 2007), and subsequently re-settled as a further quartz purification step. All of the measurements were undertaken on a single aliquot that was pre-sensitized by numerous cycles of irradiation, heating, and optical stimulation, in order to reduce the trap type variability and minimize sensitivity changes.

Luminescence measurements were performed on a Risø TL-DA-20 reader incorporating blue LEDs emitting at 470nm and delivering 50 mW/cm^2 (Bøtter-Jensen et al., 2003). The luminescence signal was recorded using an EMI9635QA photomultiplier tube equipped with 7.5 mm of U-340 filter, and a convex quartz lens to improve signal collection efficiency (giving ~75% brighter signal). A strontium/yttrium beta source with a dose rate of 0.083 Gy/s was used for laboratory irradiation, and a preheat of 260 °C for 10 s was applied to all samples before the OSL stimulations to yield the natural (L_n), regenerative (L_x) and test (T_x) dose signals. Integration intervals included the first two channels (2 s) of measurement minus a background of the last ten channels (10 s) of measurement.

3. Advances in TT-OSL measurement protocols

The basic steps of TT-OSL measurement involve an optical stimulation to empty electron traps associated with the fast component of the OSL signal, and a heat treatment to thermally transfer

electrons from other less light-sensitive traps into the fast component traps. A second optical stimulation then gives the TT-OSL signal. The original sequence proposed by Wang et al. (2006a) has been thoroughly investigated in later studies, and the measurement protocol underwent several alterations, including the transition from a multiple aliquot protocol to a single aliquot protocol within a year of publication (Wang et al., 2007).

Wang et al. (2006a) described two parts to the TT-OSL signal, the BT-OSL signal and the recuperated OSL (Re-OSL) signal. The Re-OSL signal was the target signal for dating and could be obtained by subtracting the BT-OSL signal from the entire TT-OSL signal. Division of the TT-OSL signal into two parts was based on the theoretical understanding that Re-OSL originated from a double transfer process while BT-OSL originated from a single transfer process. In a double transfer process, a proportion of the electrons in the traps associated with the OSL fast component are temporarily stored in alternative traps after eviction by the initial blue light stimulation; the subsequent thermal transfer preheat then transfers these electrons from the alternative trap back into the OSL fast component traps where they can then be measured during the second light stimulation. In a single transfer process, the thermal transfer preheat accesses electrons in alternative traps that were not originally stored in the OSL fast component traps and transfers them into those traps.

Wang et al. (2006b) hypothesized that the BT-OSL signal would originate from light-insensitive traps with long lifetimes that had been accumulating electrons for many sedimentary cycles. It was therefore expected to be a constant background signal to all TT-OSL measurements. Wang et al. (2006a) proposed that the BT-OSL signal could be measured by repeatedly heating and optically stimulating an aliquot after measuring the OSL signal; the TT-OSL signal would decrease with each heating/stimulation cycle until reaching a plateau at the level of the BT-OSL signal. However, this method of separating the signals was thought to be too time consuming for routine dating experiments, so Wang et al. (2006b) performed heating experiments and proposed that only the BT-OSL signal would remain after annealing an aliquot at 300 °C for 10s.

Later studies determined that the theoretical underpinning of the division of the TT-OSL signal was flawed. Adamiec et al. (2008) demonstrated that even the Re-OSL signal originates from a single transfer process, and Kim et al. (2009) observed that the BT-OSL signal is not constant but

rather increases with dose similarly to the TT-OSL signal. Porat et al. (2009) concluded that measurement and removal of the BT-OSL signal is not necessary when a small test dose is used. These observations and interpretations led several subsequent researchers to use TT-OSL protocols omitting measurement of the BT-OSL signal (e.g. Liu et al., 2012; Stevens et al., 2009).

The original sequence of Wang et al. (2006a) used an OSL test dose signal to normalize and correct for sensitivity changes between regenerative doses. This was practical in comparison to use of a TT-OSL test dose signal in that it requires less measurement time and has a higher signal to noise ratio; furthermore, this approach seemed appropriate given the assumption that the Re-OSL signal originated from the same traps before double transfer. The realization that TT-OSL is a single transfer process, however, raised the question of whether using a TT-OSL test dose signal would more accurately reflect sensitivity changes in the traps being used for dating. Stevens et al. (2009) were the first to suggest a TT-OSL protocol implementing a TT-OSL test dose signal, a suggestion incorporated into later protocols used by Thiel et al. (2012) and Liu et al. (2012).

However, when using a TT-OSL test dose signal, it is essential that prior to each given dose, the TT-OSL source traps must be adequately emptied so that the test dose signal is not affected by a residual regenerative dose signal. This was less of an issue for OSL test dose signals because they are significantly brighter than the TT-OSL signals, thereby making any residual signal insignificant. Various studies have suggested different means for removal of this signal using heat and light stimulations at different temperatures and durations (e.g. OSL 290 °C/400 s, Stevens et al., 2009; OSL 280 °C/300 s, Liu et al., 2012). Adamiec et al. (2010) also recommended using a TT-OSL signal-removal step (350 °C/200 s, Adamiec et al., 2010) after measuring each test dose signal in order to reduce signal build-up between regenerative doses. In order to minimize unaccounted sensitivity change, protocols frequently assign a slightly less rigorous signal-removal treatment before the test dose than before the subsequent regenerative dose (Liu et al., 2012; Stevens et al., 2009; Thiel et al., 2012).

4. TT-OSL measurement and signal

The TT-OSL protocols used in this study (Table 1) build on the discoveries and advances that have been made since its original introduction (Wang et al. 2006a). We use single aliquot protocols and TT-OSL test dose signals, but maintain the same thermal and optical stimulations of Wang et al. (2006a). For TT-OSL signal removal before the test dose and regenerative dose, we return to the original work and discussion of the BT-OSL signal (Wang et al. 2006b) by repeating ten TT-OSL signal measurement cycles. Although this process does provide a measurement of the BT-OSL signal, it is not subtracted from the TT-OSL signal measured from the first optical stimulation after the OSL fast component depletion (Fig. 1).

The protocols used in this study are labelled A-D (Table 1). Protocol A is a constant irradiation protocol, while protocols B-D are pulsed irradiation protocols. For the same regenerative dose of 1650 Gy, the four protocols differ only in how the initial 1650 Gy dose is given to the aliquot. In protocol A, the dose is given in a single irradiation step with no extra thermal treatments. Protocol B is similar to Wang et al.'s (2006a) pulsed-irradiation procedure; it divides the 1650 Gy into ten steps of 165 Gy separated by 240 °C 0 s cut-heats, and no extra thermal treatment is given after the last 165 Gy dose and before the OSL preheat (step 5, Table 1). Protocol C maintained the same thermal treatment temperature (240 °C) as protocol B, but reduced the size of each irradiation step by a factor of ten to 16.5 Gy. This alteration was made to ensure that the unstable traps affecting charge competition in the quartz do not become saturated during the irradiation step and therefore reduce the ability of the pulsed-irradiation procedure to mimic competition in nature. Protocol C used the same, small irradiation step (16.5 Gy) as protocol B, but used a lower temperature for the inter-pulse thermal treatments (160 °C). This variation was made to reduce the potential for partial annealing of higher temperature traps while still removing charge from many of the unstable traps (such as those associated with the 110 °C thermoluminescence peak).

A dose response curve was constructed using protocol A (constant-irradiation) as described in Table 1. Seven regenerative doses were used, including a zero dose. The curve, shown in figure 2, was measured from the lowest regenerative dose to the highest regenerative dose six times on a single pre-sensitized aliquot, resulting in a total of 42 measurements being used to define the curve. Each

point on the curve (Fig. 2) shows the signal intensity in response to a given laboratory dose. The signal intensities are calculated as the integrated TT-OSL regenerative dose signal (L_x) divided by the subsequent integrated TT-OSL test dose signal (T_x). A plot of the L_x/T_x values as a function of dose was fitted with a single saturating exponential function (Eqn. 1), where S is the L_x/T_x value for given regenerative dose (D), D_0 is the characteristic dose that describes the shape of the dose response curve and A is the pre-exponential factor defining the L_x/T_x value at saturation. The values of D_0 and A for the dose response curve in figure 2 are 1159 ± 54 and 5.73 ± 0.13 respectively.

$$S(D) = A(1 - \exp\left[-\frac{D}{D_0}\right]) \quad \text{Equation 1}$$

The L_x/T_x value for a natural signal (L_n/T_n) is the same regardless of whether a constant- or pulsed-irradiation protocol is used to define the laboratory dose response curve. Therefore, any difference in ages calculated using the different protocols is solely dependent on changes to the dose response curve. In this study, instead of constructing multiple dose response curves with constant- and pulsed-irradiation, we focus on a 1650 Gy dose and investigate how the L_x/T_x value for that single regeneration dose varies with constant- and pulsed-irradiation.

5. Determining the impact of heat treatments on the TT-OSL signal

In addition to comparing the measured values for different constant- and pulsed-irradiation protocols, this study investigates the existence and/or degree of partial thermal annealing of the TT-OSL signal resulting from the heat treatments between irradiation steps. To do this, the percentage signal loss was determined for temperatures of 160 and 240 °C using the same aliquot of sample PT2 that was used to construct figure 2. The aliquot was heated to 500 °C to remove any existing charge, irradiated with 1650 Gy in a single irradiation step and then given different numbers of thermal treatments before being measured using steps 2-13 of protocol A (Table 1). The number of thermal treatments varied from 0 to 10, and each number of thermal treatments was measured at least three times. The resulting L_x/T_x values (Fig. 3) demonstrate significant signal loss per thermal treatment at 240 °C, and a much lower signal loss per thermal treatment at 160 °C. By weighting the data by its relative standard errors and fitting it with decaying exponential functions, the signal loss was

calculated to be 3.31 ± 0.16 % per treatment for 240 °C heat treatments, and 0.33 ± 0.22 % per treatment for 160 °C heat treatments.

The values for the percentage signal loss per heat treatment (Fig. 3) were used in conjunction with the protocol A constant-irradiation dose response curve (Fig. 2) to calculate the 1650 Gy L_x/T_x values predicted for each of the three pulsed-irradiation protocols (B-D) as a result of partial thermal annealing of the 1650 Gy L_x signal. These calculations were made using two approaches: First, a recursive expression following the actual signal growth and loss that occurred with each irradiation step and thermal treatment (Fig. 4; zigzag black curve); and second, a closed-form expression that approximates the effective signal growth with a smooth function (Fig.4; red dashed curve).

5.1 Recursive expression

In a pulsed irradiation protocol the first irradiation step provides the aliquot with its initial signal intensity (L_x). This intensity is then decreased by a factor X (%) during the subsequent thermal treatment. Each subsequent irradiation step increases the L_x signal intensity and each subsequent thermal treatment reduces the L_x signal intensity. Note that a thermal treatment reduces the entire L_x signal accumulated and not only the part of the signal induced by the preceding irradiation step. The recursive expression follows these L_x signal intensity changes by calculating increases in signal using the fitted dose response curve and decreases in signal using the percent signal loss per thermal treatment shown in figure 3. This calculation method is mathematically based on equation 1 as well as its inverse function (Eqn 2), which calculates the absorbed radiation dose (D) corresponding to a known signal intensity (S).

$$D(S) = -D_0 \ln\left(1 - \frac{S}{A}\right) \quad \text{Equation 2}$$

The recursive formula given in equation 3 calculates the apparent absorbed dose ($D_{e,p}$) at each particular irradiation step (p) by introducing the following new variables: D_{step} (Gy) is the dose delivered at each irradiation step, X (%) is the fractional signal intensity loss due to one thermal treatment, and P is the total number of irradiation steps.

$$D_{e,0} = 0\,, \quad D_{e,p+1} = D\{S(D_{e,p} + D_{step})(1 - X)\} \quad \text{Equation 3}$$

If thermal treatments have a negligible effect on intensity, $X \sim 0$ and equation 3 simplifies to equation 4, such that the apparent absorbed dose ($D_{e,p}$) is equal to the sum of irradiation steps administered.

$$D_{e,p} = pD_{step} \quad \text{Equation 4}$$

However, when signal loss due to thermal treatment is significant ($X > 0$), the apparent dose ($D_{e,p}$) is smaller than the sum of all doses delivered, the exact difference being a function of X, p, D_{step}, and D_0.

5.2 Closed-form expression

The closed-form expression approximates the signal intensity after the final irradiation step is administered. The form of the analytical expression therefore corresponds to a saturating exponential function within the zigzag-shaped actual signal growth curve which ends at the same point (Fig. 4). It is calculated by approximating a detrapping rate (K, s^{-1}) based on thermal annealing by the thermal treatments (Eqn. 5) where X (%) is the fractional intensity loss due to one thermal treatment, $P - 1$ is the number of thermal treatments (i.e. the number of irradiation steps minus one), $\dot{D}$ is the laboratory beta source dose rate (Gy/s), and $D_e/\dot{D}$ is the time (in seconds) required to deliver the total dose (D_e) to the sample.

$$K = \frac{X(P-1)}{D_e/\dot{D}} \quad \text{Equation 5}$$

The increase in signal intensity over time can then be calculated as the electron trapping rate per second (D_e/D_0) times the number of available traps (N-n, where N is the total number of electron traps and n is the number of traps currently filled) minus the detrapping rate (K, s^{-1}) times the number of filled traps (n, Eqn. 6).

$$\frac{dn}{dt} = \frac{\dot{D}}{D_0}(N - n) - Kn \quad \text{Equation 6}$$

As outlined by Guralnik et al. (2013) the apparent age (t_{app}) in such a system can be calculated by the following expression:

$$t_{app} = \frac{D_e}{\dot{D}} = \frac{-1}{\dot{D}/D_0 + K} \ln\left[1 - \left(\frac{n}{N}\right)\left(\frac{\dot{D}/D_0 + K}{\dot{D}/D_0}\right)\right] \quad \text{Equation 7}$$

The saturation level (n/N) for a system that has been given a known dose D_e under known trapping ($\dot{D}/D_0$) and detrapping (K) rates (s^{-1}) can then be determined by rearranging equation 7 to equation 8 and the L_x/T_x intensity (S) can be calculated by multiplying the saturation level (n/N) by the pre-exponential factor (A) of the dose response curve.

$$\frac{n}{N} = \frac{\dot{D}/D_0}{\dot{D}/D_0+K}\left\{1 - \exp\left[-D_e\left(\frac{1}{D_0} + \frac{K}{\dot{D}}\right)\right]\right\} \quad \text{Equation 8}$$

$$S = A\left(\frac{n}{N}\right) \quad \text{Equation 9}$$

5.3 Expression intercomparison

Solutions from the recursive and closed-form expressions provide the same L_x/T_x value predictions (reported in section 6) further validating the results obtained by each expression separately. Although the recursive expression follows the pulsed irradiation protocol step by step, the closed-form function of equation 8 offers a conceptual expression for understanding the interchangeable effects of signal depletion due to a single thermal treatment (X) and the number of pulsed-irradiation steps (P). This expression could be used to predict the impact of any pulsed irradiation procedure so long as the parameters (K, $\dot{D}$, D_0, A) are known.

6. Results

The results of this pulsed irradiation investigation include the observed difference in outcome between L_x/T_x values for constant- and pulsed-irradiation protocols, and an assessment of the proportion of the difference in outcome that can be explained by partial thermal annealing. Results of the different pulsed-irradiation protocols (B-D) are compared to results of the constant-irradiation protocol A in figure 5. The dark-coloured (red) bars representing the constant-irradiation results (Protocol A, Fig. 5a) are repeated in each subfigure (Fig. 5b-5d) behind the light grey bars of the pulsed-irradiation protocols results for easy comparison. The L_x/T_x value for 1650 Gy was measured with protocol A nine times, and the weighted mean was calculated to be 4.34 ± 0.11 (Fig. 5a). Each of the three pulsed-irradiation protocols was measured six times. Protocol B, which mimics the procedure used by Wang et al. (2006a) (240 °C thermal treatments and 165 Gy irradiation steps), had a weighted mean L_x/T_x value of 3.64 ± 0.11 (Fig. 5b), while protocol C (using 240 °C thermal

treatments and 16.5 Gy irradiation steps) had a weighted mean L_x/T_x value of 2.37 ± 0.11 (Fig. 5c). Protocol D used a less stringent 160 °C thermal treatment and a 16.5 Gy pulse dose; this gave a weighted mean L_x/T_x value of 4.14 ± 0.13 (Fig. 5d).

Evidence of the dependence of pulsed-irradiation protocol outcome on partial thermal annealing during inter-step thermal treatments is given by the extent to which differences in outcome between protocols A-D can be explained by partial annealing. In this study, this assessment is made through comparison of the observed protocol results and the results predicted due to partial thermal annealing (section 5). Note that these predicted values only account for protocol outcome differences due to signal loss during the inter-step thermal treatments and do not account for differences due to charge competition and other pulsed irradiation effects.

The predicted L_x/T_x values due to partial thermal annealing as calculated with both recursive and analytical expressions are 4.36 ± 0.31, 3.90 ± 0.37, 1.73 ± 0.25, and 3.88 ± 0.83 for protocols A, B, C, and D respectively, and are shown in figure 5 as black points with error bars facilitating comparison to the measured values in the white points and light grey histogram bars. In each case (Fig 5b-d), the expected L_x/T_x results are within error of the observed results with no obvious systematic difference that could be attributed to other influences of pulsed-irradiation such as charge distribution competition effects. The results of this study therefore suggest that the majority of the difference in outcome between constant-and pulsed-irradiation TT-OSL protocols is due to partial thermal annealing effects.

7. Discussion

Comparison of the observed and predicted L_x/T_x values for constant- and pulsed-irradiation TT-OSL protocols makes it apparent that partial annealing of the TT-OSL signal accounts for the majority of the difference in outcome observed between the protocols. The percentage TT-OSL signal loss per thermal treatment is significant, especially for the higher temperature preheat of 240 °C. Ninety-nine inter-step heat treatments of 160 °C result in similar L_x/T_x values to nine 240 °C treatments, an observation that is predicted by the expected L_x/T_x value, but would not have been expected if competition effects were responsible for most of the difference in outcome between

constant- and pulsed-irradiation protocols. It is still possible that charge competition is affected by pulsed irradiation protocols, but since any competition effects in this sample are either negligible or self-cancelling, it cannot be determined whether such effects would have more influence on unstable recombination centres or on unstable electron traps.

The observation that pulsed-irradiation protocols partially anneal the TT-OSL signal is consistent with investigations of the thermal stability of the signal. Laboratory studies have demonstrated that the TT-OSL signal is significantly less stable than the fast component OSL signal (Adamiec et al., 2010). These findings are supported by a study of coastal deposits comparing TT-OSL ages with 290 °C post IR-IRSL feldspar ages, where TT-OSL equivalent dose underestimations were observed for older samples (Thiel et al., 2012). The relatively low thermal stability of the TT-OSL signal compared to the fast component OSL and post IR-IRSL signals results in signal loss during burial for older samples due to the shorter signal lifetime at natural burial temperatures (Duller and Wintle, 2012). As pulsed-irradiation was first introduced for use with the more thermally stable fast component OSL signal, the influence of pulsed-irradiation protocols for the fast component OSL signal cannot be surmised from this study.

Because pulsed-irradiation partially anneals the TT-OSL signal, a range of age estimates can be obtained for any given sample by varying the number and temperature of thermal treatments in a pulsed irradiation protocol. Partial thermal annealing during these various thermal treatments will distort the laboratory dose response curve while leaving the natural dose unaffected resulting in a range of equivalent dose estimates. The range of age estimates obtainable from various pulsed irradiation protocols will likely include the true burial age of a sample, but the pulsed-irradiation procedure necessary to obtain the true burial age cannot typically be determined for a sample of unknown age. Hence the observation of TT-OSL ages in agreement with Ar-Ar ages for the samples taken near the B/M boundary by Wang et al. (2006a) may have been a fortuitous coincidence in which the pulsed-irradiation protocol annealed a comparable amount of signal to that which was removed temporally during burial.

8. Conclusions

Differences in equivalent dose values obtained using constant- and pulsed-irradiation TT-OSL protocols in this study are primarily the result of pulsed-irradiation inter-step heat treatments partially annealing the TT-OSL signal. Any net impact of pulsed-irradiation on TT-OSL charge competition was of too low a magnitude to have been observed. Partial thermal annealing during inter-step thermal treatments distorts the laboratory dose response curve while leaving the natural signal unaffected. This suggests that a pulsed-irradiation TT-OSL protocol could be able to provide an accurate age estimate for an older sample by thermally annealing the same amount of signal that decayed temporally in nature due to the short lifetime of the TT-OSL signal. As the amount of signal loss in nature is dependent on the age of a sample, which is usually unknown, the correct pulsed-irradiation protocol required to compensate for such signal loss cannot typically be determined. Therefore, pulsed-irradiation TT-OSL protocols will result in age estimates that are older than those derived using constant-irradiation protocols, but that are unreliable. Future studies implementing pulsed-irradiation procedures may investigate and compensate for charge competition effect differences, but such studies will need to assess and account for the degree of partial annealing by the inter-step thermal treatments.

Acknowledgements

This material is based upon work supported by the National Science Foundation Graduate Research Fellowship under Grant No. 1053735 to MSC. Additional support for MSC is provided by Aberystwyth University. HMR acknowledges a Leverhulme grant awarded to Prof. B.A. Maher (Lancaster University) which made it possible to collect the sample. Aberystwyth Luminescence Research Laboratory (ALRL) benefits from being part of the Climate Change Consortium of Wales (C3W).

Christina Ankjaergaard is thanked for refereeing this paper and improving its clarity. The mathematical explanation in section 5 was greatly improved by the suggestions of the second reviewer, Benny Guralnik and he is thanked for this as well as for suggesting the closed-form analytical approach.

References

Adamiec, G., Bailey, R.M., Wang, X.L., Wintle, A.G., 2008. The mechanism of thermally transferred optically stimulated luminescence in quartz. Journal of Physics D: Applied Physics 41, 135503.

Adamiec, G., Duller, G.A.T., Roberts, H.M., Wintle, A.G., 2010. Improving the TT-OSL SAR protocol through source trap characterisation. Radiat Meas 45, 768-777.

Bailey, R.M., 2004. Paper I--simulation of dose absorption in quartz over geological timescales and its implications for the precision and accuracy of optical dating. Radiat Meas 38, 299-310.

Bøtter-Jensen, L., Andersen, C.E., Duller, G.A.T., Murray, A.S., 2003. Developments in radiation, stimulation and observation facilities in luminescence measurements. Radiat Meas 37, 535-541.

Coe, R.S., Singer, B.S., Pringle, M.S., Zhao, X., 2004. Matuyama–Brunhes reversal and Kamikatsura event on Maui: paleomagnetic directions, 40Ar/39Ar ages and implications. Earth and Planetary Science Letters 222, 667-684.

Duller, G.A.T., Wintle, A.G., 2012. A review of the thermally transferred optically stimulated luminescence signal from quartz for dating sediments. Quat Geochronol 7, 6-20.

Guralnik, B., Jain, M., Herman, F., Paris, R.B., Harrison, T.M., Murray, A.S., Valla, P.G., Rhodes, E.J., 2013. Effective closure temperature in leaky and/or saturating thermochronometers. Earth and Planetary Science Letters 384, 209-218.

Kim, J.C., Duller, G.A.T., Roberts, H.M., Wintle, A.G., Lee, Y.I., Yi, S.B., 2009. Dose dependence of thermally transferred optically stimulated luminescence signals in quartz. Radiat Meas 44, 132-143.

Liu, J., Murray, A.S., Jain, M., Buylaert, J.-P., Lu, Y., Chen, J., 2012. Developing a SAR TT-OSL protocol for volcanically-heated aeolian quartz from Datong (China). Quat Geochronol.

Pickering, R., Jacobs, Z., Herries, A.I.R., Karakanas, P., Bar-Mathews, M., Woodhead, J.D., Kappen, P., Fisher, E., Marean, C.W., 2013. Paleoanthropologically significant South African sea caves dated to 1.1-1.0 million years using a combination of U-Pb, TT-OSL and palaeomagnetism. Quaternary Science Reviews 65, 39-52.

Porat, N., Duller, G.A.T., Roberts, H.M., Wintle, A.G., 2009. A simplified SAR protocol for TT-OSL. Radiat Meas 44, 538-542.

Qin, J.T., Zhou, L.P., 2009. Stepped-irradiation SAR: A viable approach to circumvent OSL equivalent dose underestimation in last glacial loess of northwestern China. Radiat Meas 44, 417-422.

Roberts, H.M., 2007. Assessing the effectiveness of the double-SAR protocol in isolating a luminescence signal dominated by quartz. Radiat Meas 42, 1627-1636.

Stevens, T., Buylaert, J.P., Murray, A.S., 2009. Towards development of a broadly-applicable SAR TT-OSL dating protocol for quartz. Radiat Meas 44, 639-645.

Thiel, C., Buylaert, J.-P., Murray, A.S., Elmejdoub, N., Jedoui, Y., 2012. A comparison of TT-OSL and post-IR IRSL dating of coastal deposits on Cap Bon peninsula, north-eastern Tunisia. Quat Geochronol.

Wang, X.L., Lu, Y.C., Wintle, A.G., 2006a. Recuperated OSL dating of fine-grained quartz in Chinese loess. Quat Geochronol 1, 89-100.

Wang, X.L., Wintle, A.G., Lu, Y.C., 2006b. Thermally transferred luminescence in fine-grained quartz from Chinese loess: Basic observations. Radiat Meas 41, 649-658.

Wang, X.L., Wintle, A.G., Lu, Y.C., 2007. Testing a single-aliquot protocol for recuperated OSL dating. Radiat Meas 42, 380-391.

Figure Captions

1. Signal intensities of the OSL and TT-OSL signals in response to a dose of 165 Gy. The first decay is the 300 s OSL signal and the second (highlighted) is the 100 s TT-OSL signal used for dating. Signals are separated by heating to 260 °C for 10 s.
2. TT-OSL dose response curve using protocol A (constant-irradiation). The points are fitted with a single saturating exponential of the form: $L_x/T_x = 5.7 * (1-\exp(-D/1160))$. Dashed lines depict 95% confidence intervals. Relative standard deviations of the L_x/T_x values range from 10% at lower doses to 5% at higher doses, with the lower doses having more scatter due to lower signal intensity.
3. Plot of L_x/T_x values against the number of thermal treatments given before measurement. Each point is a weighted mean and standard error of at least three measurements. Solid curves are error-weighted fits of decaying exponential functions. Dashed lines depict 95% confidence intervals.
4. Conceptual diagram of the analytical and recursive expressions for calculating the L_x/T_x values expected for a pulsed irradiation protocol. Example curves are based on 1650 Gy dose given in 10 irradiation steps with 10% signal loss during each thermal treatment.
5. Histograms for the each of the four TT-OSL protocols used in this study. Dark (red) histograms represent constant-irradiation while light grey histograms represent pulsed-irradiation. The black points and error bars show the estimated signal due solely to partial annealing. Subfigures 5b and 5c show histograms for protocols with 240 °C thermal treatments, and subfigures 5c and 5d show histograms for protocols with 16.5 Gy pulse doses.

Table Captions

1. TT-OSL measurement protocols used in this study

Figure 1:

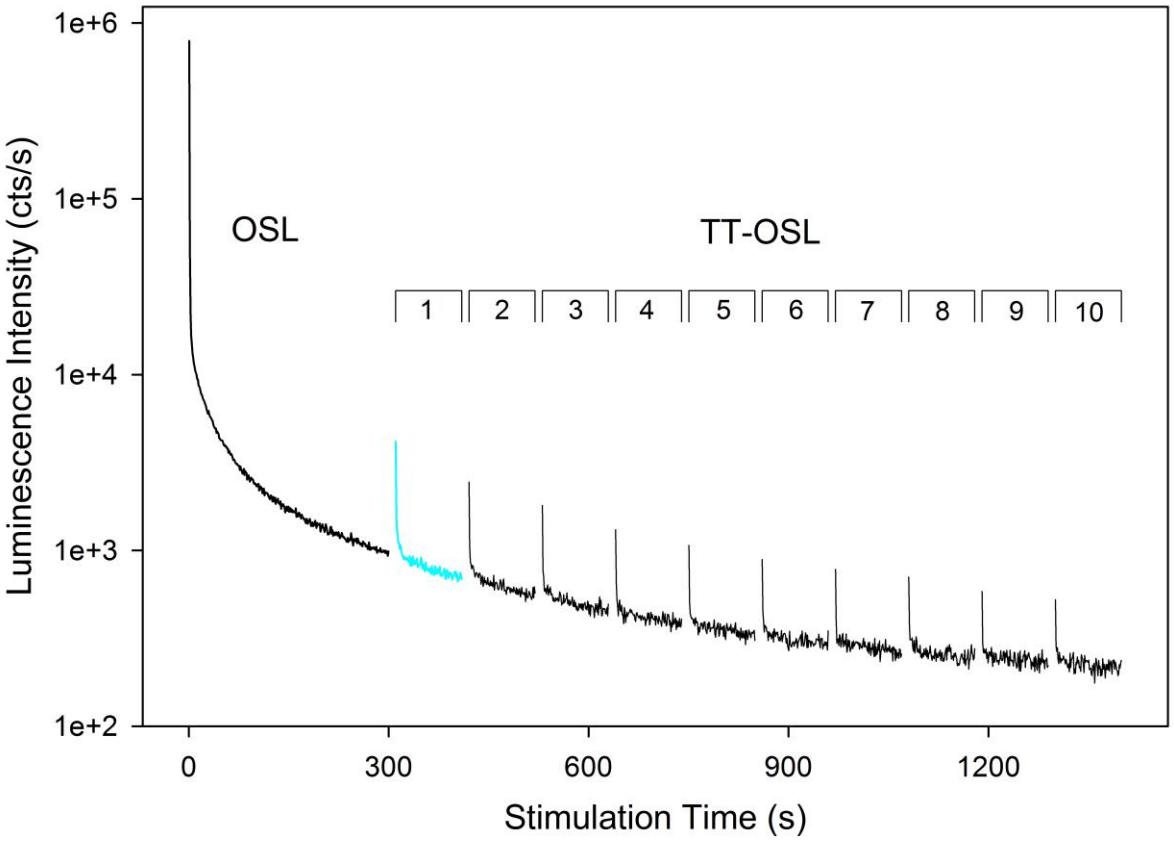

Figure 2:

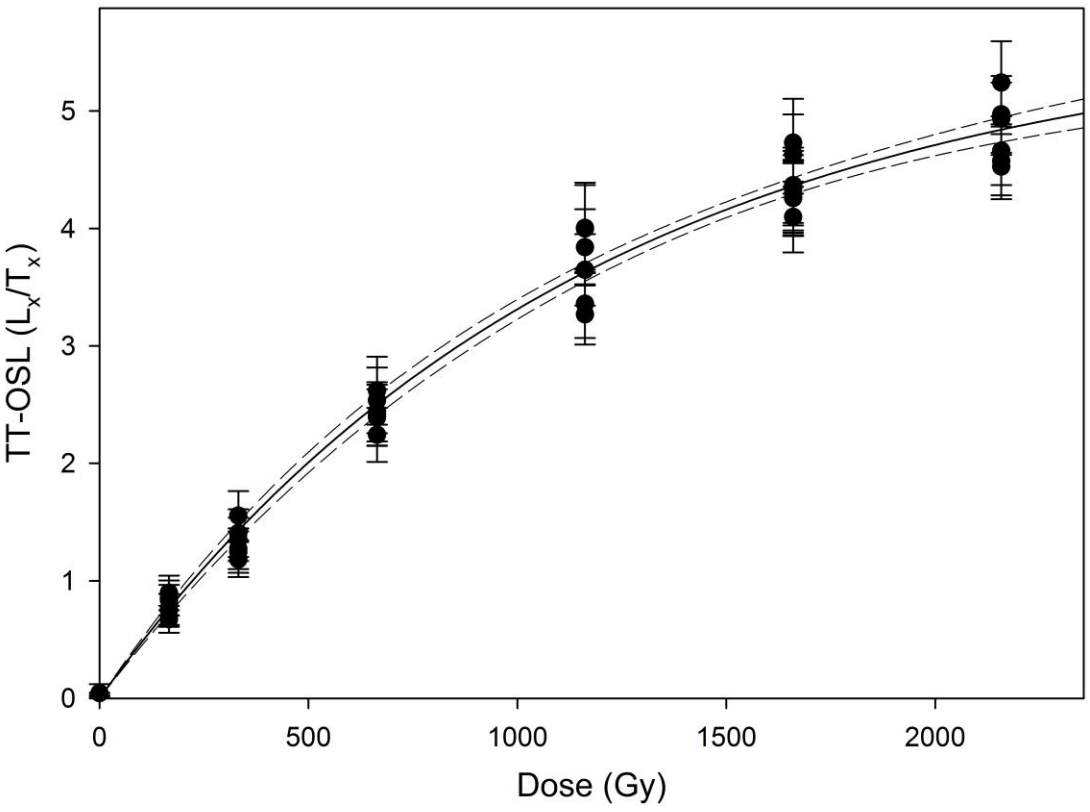

Figure 3:

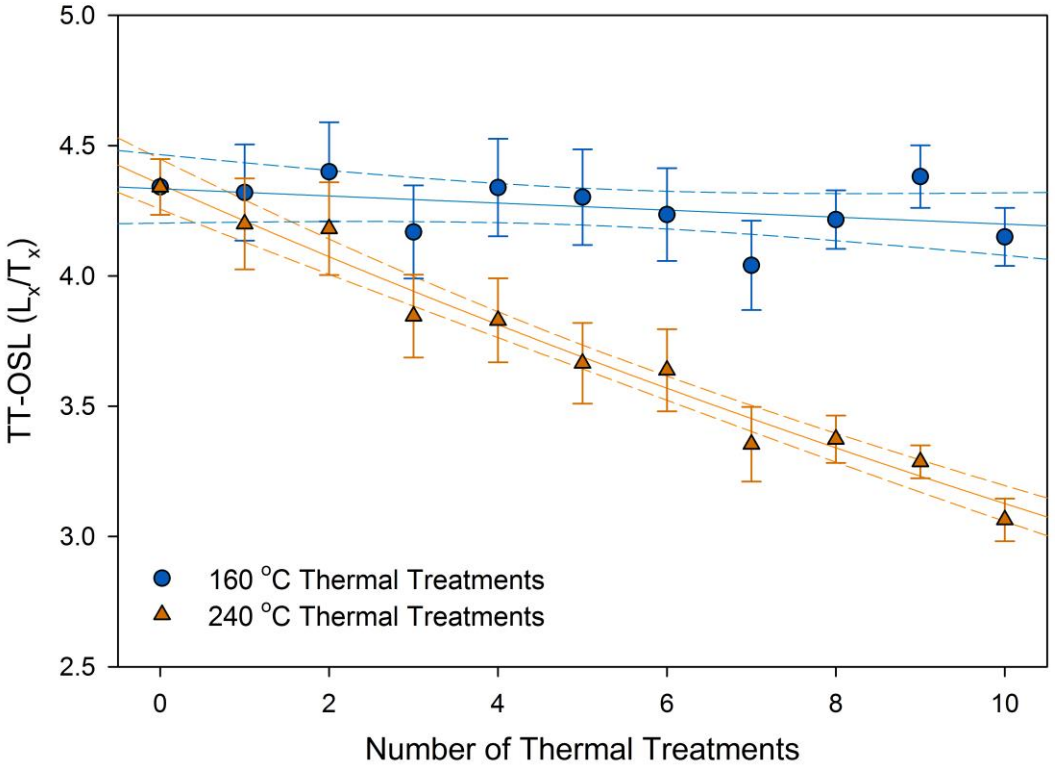

Figure 4:

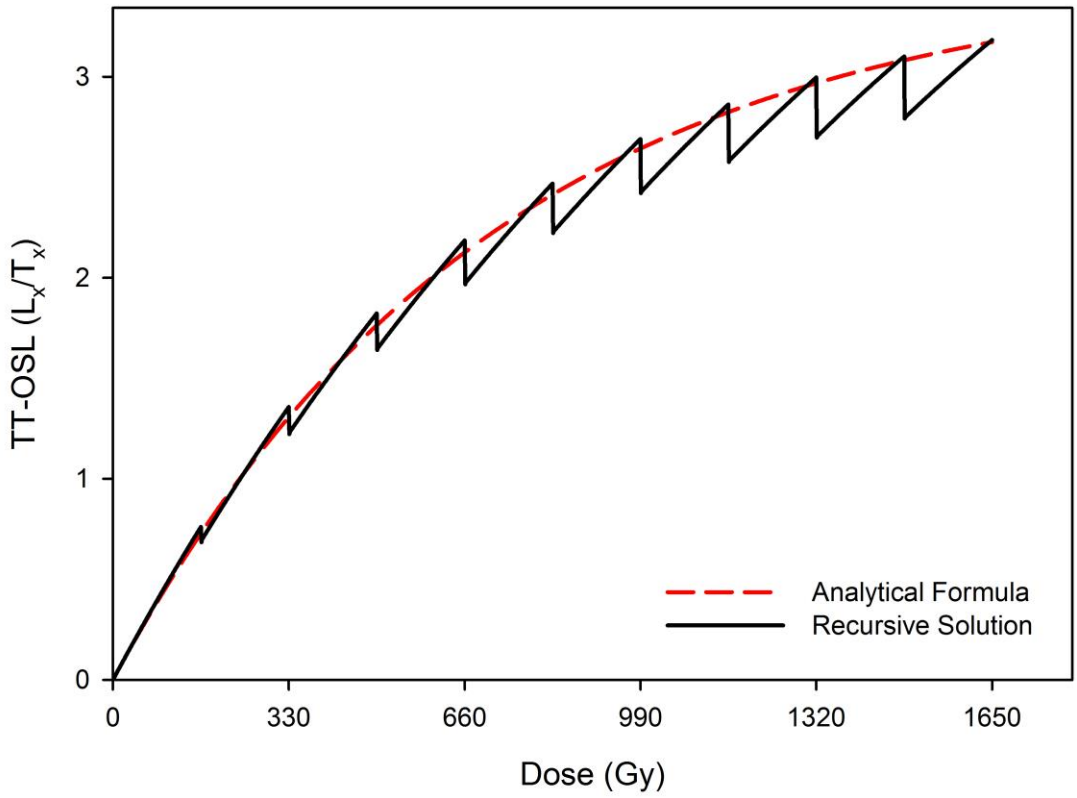

Figure 5:

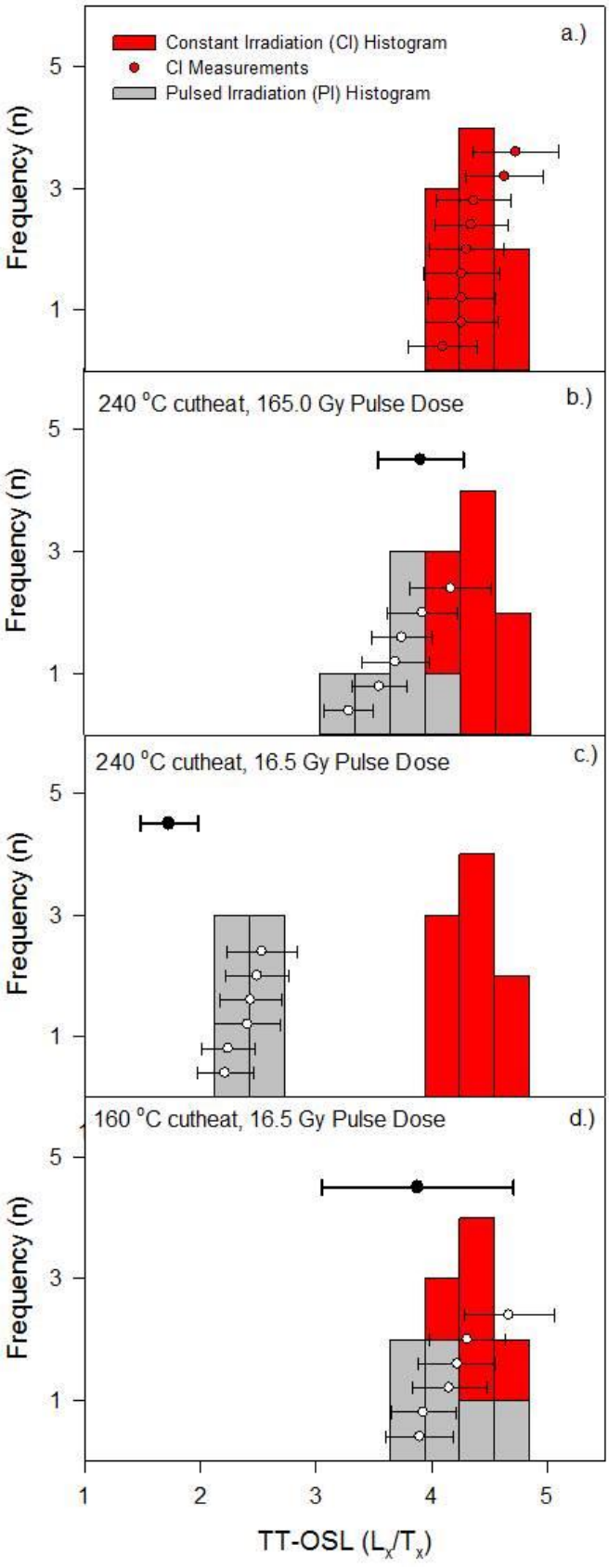
a.)
Constant Irradiation (CI) Histogram
CI Measurements
Pulsed Irradiation (PI) Histogram
b.)
240 °C cutheat, 165.0 Gy Pulse Dose
c.)
240 °C cutheat, 16.5 Gy Pulse Dose
d.)
160 °C cutheat, 16.5 Gy Pulse Dose
Frequency (n)
TT-OSL (L$_x$/T$_x$)

Table 1:

	A.	B.	C.	D.
1	1650 Gy Dose	165 Gy Dose	16.5 Gy Dose	16.5 Gy Dose
2	Preheat 260 °C/ 10 s	240 °C cut heat	240 °C cut heat	160 °C cut heat
3	OSL 125 °C/ 300 s	Repeat 1-2 eight times	Repeat 1-2 ninety-eight times	Repeat 1-2 ninety-eight times
4	Preheat 260 °C/ 10 s	165 Gy Dose	16.5 Gy Dose	16.5 Gy Dose
5	OSL 125 °C/ 100 s (L_x)	Preheat 260 °C/ 10 s	Preheat 260 °C/ 10 s	Preheat 260 °C/ 10 s
6	Repeat 4-5 nine times	OSL 125 °C/ 300 s	OSL 125 °C/ 300 s	OSL 125 °C/ 300 s
7	165 Gy Dose	Preheat 260 °C/ 10 s	Preheat 260 °C/ 10 s	Preheat 260 °C/ 10 s
8	Preheat 260 °C/ 10 s	OSL 125 °C/ 100 s (L_x)	OSL 125 °C/ 100 s (L_x)	OSL 125 °C/ 100 s (L_x)
9	OSL 125 °C/ 300 s	Repeat 7-8 nine times	Repeat 7-8 nine times	Repeat 7-8 nine times
10	Preheat 260 °C/ 10 s	165 Gy Dose	165 Gy Dose	165 Gy Dose
11	OSL 125 °C/ 100 s (T_x)	Preheat 260 °C/ 10 s	Preheat 260 °C/ 10 s	Preheat 260 °C/ 10 s
12	Repeat 10-11 nine times	OSL 125 °C/ 300 s	OSL 125 °C/ 300 s	OSL 125 °C/ 300 s
13	Preheat 500 °C/ 0 s	Preheat 260 °C/ 10 s	Preheat 260 °C/ 10 s	Preheat 260 °C/ 10 s
14		OSL 125 °C/ 100 s (T_x)	OSL 125 °C/ 100 s (T_x)	OSL 125 °C/ 100 s (T_x)
15		Repeat 10-11 nine times	Repeat 10-11 nine times	Repeat 10-11 nine times
16		Preheat 500 °C/ 0 s	Preheat 500 °C/ 0 s	Preheat 500 °C/ 0 s